1-1-2012

High strength thin-walled rectangular concrete-filled tubular slender beam-columns, Part II: Behaviour

Muhammad N. S Hadi
University of Wollongong, mhadi@uow.edu.au

Qing Quan Liang
Victoria University

Vipulkumar I. Patel
Victoria University, Melbourne

Manuscript prepared for

Journal of Constructional Steel Research

April 2011

High Strength Thin-Walled Rectangular Concrete-Filled Steel Tubular Slender Beam-Columns, Part II: Behavior

Vipulkumar Ishvarbhai Patel[a], Qing Quan Liang[a,*], Muhammad N. S. Hadi[b]

[a]School of Engineering and Science, Victoria University, PO Box 14428, Melbourne, VIC 8001, Australia

[b]School of Civil, Mining and Environmental Engineering, University of Wollongong, Wollongong, NSW 2522, Australia

Corresponding author:

Dr. Qing Quan Liang
School of Engineering and Science
Victoria University
PO Box 14428
Melbourne VIC 8001
Australia
Phone: +61 3 9919 4134
Fax: +61 3 9919 4139
E-mail: Qing.Liang@vu.edu.au

High strength thin-walled rectangular concrete-filled steel tubular slender beam-columns, Part II: Behavior

Vipulkumar Ishvarbhai Patel[a], Qing Quan Liang[a,*], Muhammad N. S. Hadi[b]

[a]*School of Engineering and Science, Victoria University, PO Box 14428, Melbourne, VIC 8001, Australia*
[b]*School of Civil, Mining and Environmental Engineering, University of Wollongong, Wollongong, NSW 2522, Australia*

ABSTRACT

Experimental and numerical research on full-scale high strength thin-walled rectangular steel slender tubes filled with high strength concrete has not been reported in the literature. In a companion paper, a new numerical model was presented that simulates the nonlinear inelastic behavior of uniaxially loaded high strength thin-walled rectangular concrete-filled steel tubular (CFST) slender beam-columns with local buckling effects. The progressive local and post-local buckling of thin steel tube walls under stress gradients was incorporated in the numerical model. This paper presents the verification of the numerical model developed and its applications to the investigation into the fundamental behavior of high strength thin-walled CFST slender beam-columns. Experimental ultimate strengths and load-deflection responses of CFST slender beam-columns tested by independent researchers are used to verify the accuracy of the numerical model. The verified numerical model is then utilized to investigate the effects of local buckling, column slenderness ratio, depth-to-thickness ratio, loading eccentricity ratio, concrete compressive strengths and steel yield strengths on the behavior of high strength thin-walled CFST slender beam-columns. It is demonstrated that the numerical

* Corresponding author: Tel.: +61 3 9919 4134; Fax: +61 3 9919 4139
E-mail address: Qing.Liang@vu.edu.au

model is accurate and efficient for determining the behavior of high strength thin-walled CFST slender beam-columns with local buckling effects. Numerical results presented in this study are useful for the development of composite design codes for high strength thin-walled rectangular CFST slender beam-columns.

Keywords: Concrete-filled steel tubes; High strength materials; Local and post-local buckling; Nonlinear analysis; Slender beam-columns.

1. Introduction

High strength concrete and high strength steel tubes are increasing used in construction of concrete-filled steel tubular (CFST) slender beam-columns which are widely used in high rise composite buildings. The use of high strength thin-walled steel tubes and high strength concrete can reduce the cross-sectional area of rectangular CFST slender beam-columns. Thin-walled steel tubes filled with concrete under axial load and bending are subjected to stress gradients which may cause local buckling. The strength and ductility of a rectangular CFST beam-column is considerably reduced due to local buckling. Therefore, local buckling effects must be taken into account in order to accurately predict the ultimate strength of a thin-walled high strength rectangular CFST beam-column. Design codes such as Eurocode 4 [1], LRFD [2] and ACI 318-05 [3] limit the use of structural steels with yield strength higher than 460 MPa and concrete with the compressive strength higher than 50 MPa in composite columns due to a lack of research on high strength CFST columns. Experiments on full-scale high strength rectangular CFST slender beam-columns are very expensive and time consuming. On the other hand, numerical modeling techniques can compensate the drawbacks

of experiments and can be used to investigate the behavior of full-scale high strength CFST slender beam-columns with a wide range of parameters.

The experimental behavior of rectangular CFST slender beam-columns has been studied by various researchers. Bridge [4] conducted experiments on square CFST slender beam-columns under axial load and uniaxial bending. Test specimens were constructed by normal strength steel tubes and concrete. Shakir-Khalil and Zeghiche [5] tested cold-formed steel tubes with yield strength of 386 MPa filled with normal strength concrete. An experiment study on normal strength CFST slender beam-columns was carried out by Matsui et al. [6]. These columns were constructed by filling normal strength concrete into cold-formed steel tubes. Chung et al. [7] tested eight high strength CFST slender beam-columns under axial loads and uniaxial bending. Test specimens were made of high strength concrete with compressive strength of 94.1 MPa and steel tubes with yield strength of 450 MPa. Experiments were conducted by Vrcelj and Uy [8] to examine the behavior of high strength CFST slender beam-columns. High strength concrete was filled into the cold-formed steel tubes to construct the test specimens. Zhang et al. [9] experimentally studied the strengths of axially and eccentrically loaded square CFST slender beam-columns made of high strength concrete and cold-formed steel tubes. It can be seen from the past experiments that the behavior of high strength thin-walled steel tubular slender beam-columns filled with high strength concrete has not been investigated.

Numerical models have been developed and used to study the behavior of CFST slender beam-columns. Vrcelj and Uy [8] investigated the effects of compressive strengths, steel yield strengths and column slenderness on the ultimate strengths of high strength square CFST slender beam-columns under eccentric loading using a numerical model that did not account

for local buckling of steel tube walls under stress gradients. Lakshmi and Shanmugam [10] examined the accuracy of their semi-analytical model that did not incorporate local buckling effects by comparisons of computational and experimental ultimate strengths of rectangular CFST slender beam columns under biaxial bending. However, the axial load-moment interaction diagrams for high strength rectangular CFST slender beam-columns have not been studied by Vrcelj and Uy [8] and Lakshmi and Shanmugam [10]. Liang [11, 12] utilized his performance-based analysis technique to investigate the effects of local buckling, concrete compressive strengths, steel yield strengths, steel ratio, and depth-to-thickness ratio (D/t) on the load-strain, moment-curvature and axial load-moment interaction curves for rectangular thin-walled CFST short beam-columns under axial load and biaxial bending. Liang [13, 14] developed new numerical models for predicting the axial load-deflection and axial load-moment interaction diagrams for high strength circular CFST slender beam-columns under axial load and bending.

It has been demonstrated that the axial load-deflection and axial load-moment interaction behavior of full-scale high strength thin-walled rectangular steel tubular slender beam-columns filled with high strength concrete has not been studied experimentally and numerically. A new numerical model for uniaxially loaded high strength thin-walled rectangular CFST slender beam-columns with local buckling effects has been presented in a companion paper [15]. This paper presents the verification of the numerical model and an investigation into the fundamental behavior of high strength CFST slender beam-columns with local buckling effects. Firstly, the numerical model is verified against existing experimental results. An extensive parametric study is then undertaken to investigate the effects of local buckling, column slenderness ratio, depth-to-thickness ratio, eccentricity ratio,

concrete compressive strengths and steel yield strengths. Finally, results obtained from parametric studies are discussed.

2. Verification of the numerical model

The efficiency and accuracy of the developed numerical model are demonstrated through comparisons between the numerical and existing experimental results for a large number of slender beam-column tests with different parameters. The ultimate axial and bending strengths and load-deflection curves of CFST slender beam-columns are considered in the verification of the numerical model developed.

2.1 Ultimate axial strengths of normal strength CFST columns

The geometry, material properties and experimental results of normal strength CFST slender columns tested by various researchers are given in Table 1. Specimens SCH-1, SCH-2 and SCH-7 were tested by Bridge [4]. The width (B) of the steel tubes varied between 152.5 mm and 204.0 mm while the depth (D) of the steel tubes ranged from 152.3 to 203.9 mm. The depth-to-thickness ratios (D/t) ranged from 20 to 24 while the length of the columns was either 2130 mm or 3050 mm. Specimen SCH-2 was tested under a concentric axial load. Initial geometric imperfections (u_o) at the mid-height of the specimens were measured as shown in Table 1. The axial load was applied at an eccentricity (e) of either 38 mm or 64 mm. The slender beam-columns were constructed by steel tubes filled with normal strength concrete of either 29.9 or 31.1 MPa. The steel yield strengths (f_{sy}) varied between 254 MPa and 291 MPa. The ultimate tensile strength (f_{su}) of steel tubes was assumed to be 410 MPa. The Young's modulus (E_s) of the steel material was 205 GPa.

Specimens R1, R2 and R5 shown in Table 1 were tested by Shakir-Khalil and Zeghiche [5]. These slender beam-columns with a cross-section of 80 × 120 mm were constructed by cold-formed steel tubes filled with normal strength concrete. The yield strength of the steel tubes ranged from 343.3 MPa to 386.3 MPa while the compressive strength of concrete varied between 34 MPa and 37.4 MPa. Specimens were fabricated from 5 mm thick steel tubes so that their depth-to-thickness ratio (D/t) was 24. The effective buckling lengths of the beam-columns were 3210 mm and 2940 mm about the major and minor axes respectively. The ultimate tensile strength of these steel tubes was assumed to be 430 MPa. Specimen R1 was tested under a concentric axial load while other specimens were tested under eccentric loads about either the major or minor axis. The loading eccentricity ratios (e/D) were in the range of 0.0 to 0.5. The initial geometric imperfections of specimens were not measured. Shakir-Khalil and Zeghiche [5] realized that the tested columns had initial geometric imperfections that should be recorded before testing. Therefore, the initial geometric imperfections of $L/1000$ at the mid-height of the columns were taken into account in the present numerical analysis.

Slender columns tested by Matsui et al. [6] were also considered in this study. Test parameters of specimens designated by series S1 to S12 are presented in Table 1. The columns had a square cross-section of 149.8 mm wide and 4.27 mm thick. Steel tubes with yield strength of 445 MPa were filled with normal strength concrete of 31.9 MPa. The eccentricity of the applied axial load varied from zero to a maximum of 125 mm. The length of the columns varied from 600 mm to 4500 mm covering a wide range of column slenderness. However, only slender columns were considered in this paper. Specimens S1, S5 and S9 were tested under concentric axial loads. Experimental and analytical studies conducted by Matsui et al. [6] indicated that these specimens had significant geometric

imperfections that were not recorded. The initial geometric imperfections of $L/1000$ at the mid-height of the tested specimens were considered in the present numerical analysis of these specimens.

The load-deflection analysis procedure developed by Patel et al. [15] was used to predict the ultimate strengths of these tested specimens. Test results indicated that specimen R1 did not attain its ultimate strength so that the measured maximum compressive concrete strain was used in the numerical analysis to determine the maximum load. The computational and experimental ultimate axial strengths of normal strength CFST slender beam-columns are given in Table 1, where $P_{u.\exp}$ represents the experimental ultimate axial strength and $P_{u.\text{num}}$ denotes the ultimate axial strength predicted by the numerical model. It can be seen from Table 1 that the predicted ultimate axial strengths of tested specimens are in good agreement with experimental results. The mean ultimate axial strength predicted by the numerical model is 1.03 times the experimental value with a standard deviation of 0.03 and a coefficient of variation of 0.03.

2.2 Ultimate axial strengths of high strength CFST columns

Table 2 presents the geometries, material properties and experimental results of high strength CFST slender columns tested by independent researchers. Chung et al. [7] tested a number of high strength CFST slender beam-columns subjected to axial load and uniaxial bending. The specimens were designated by series C18, C24 and C30. The lengths of specimens C18, C24 and C30 were 2250, 3000 and 3750 mm respectively. All specimens had a square cross-section of 125×125 mm. The steel tubes with yield strength of 450 MPa were filled with high strength concrete of 94.1 MPa. The tensile strength of the steel tubes was measured as 528

MPa. The depth-to-thickness ratio (D/t) of these specimens was 39. Specimens C30-0 was tested under a concentric axial load while other columns were subjected to axial loads at an eccentricity of either 20.5 mm or 61.5 mm.

Specimens CCH1, CCH2, CCM1 and CCM2 shown in Table 2 were tested by Vrcelj and Uy [8]. These columns were made of hot-rolled steel tubes which were cut into 1770 mm length. In order to simulate pinned-end support conditions, the specimen was provided with special knife-edge supports secured at their ends. The loading eccentricity ratio (e/D) was approximately equal to 0.05. The concrete compressive strength was either 52 MPa or 79 MPa while the steel yield strength was either 400 MPa or 450 MPa.

The load-deflection analysis procedure [15] was used to determine the ultimate axial strengths of these high strength specimens tested. The initial geometric imperfections of these high strength CFST slender beam-columns were not measured. However, real CFST slender beam-columns particularly small-scale ones usually have initial geometric imperfections. Therefore, the initial geometric imperfections of $L/1000$ at the mid-height of the columns were taken into account in the present numerical analysis of these columns. The ultimate axial strengths of these specimens obtained from the numerical analysis and experiments are given in Table 2. It is seen that the numerical model predicts very well the ultimate axial strengths of high strength CFST slender beam-columns. The ratio of the mean ultimate axial strength computed by the numerical model to the experimental value is 1.01. The standard deviation of $P_{u.\mathrm{num}}/P_{u.\mathrm{exp}}$ is 0.07 and the coefficient of variation is 0.07.

2.3 Ultimate bending strengths

Experimental results presented by Bridge [4], Shakir-Khali and Zeghiche [5], Matsui et al. [6] and Chung et al. [7] were used to examine the accuracy of the axial-load moment interaction strength analysis program [15]. The initial geometric imperfections of $L/1000$ at the mid-height of the columns were taken into account in the analysis of the specimens tested by Shakir-Khali and Zeghiche [5], Matsui et al. [6] and Chung et al. [7]. The ultimate axial loads obtained from experiments were applied in the numerical analysis to determine the ultimate bending strengths. The experimental and numerical ultimate bending strengths are presented in Table 3. The experimental ultimate bending strength $M_{n.\exp}$ was calculated as $M_{n.\exp} = P_{n.\exp} \times e$. It appears from Table 3 that the numerical model yields accurate predictions of the ultimate bending strengths of high strength CFST slender beam-columns. The ratio of the mean ultimate bending strength computed by the numerical model to the experimental value is 1.03 with the standard deviation of 0.05 and the coefficient of variation of 0.05.

2.4 Load-deflection curves

The load-deflection curves for CFST slender beam-columns predicted by the numerical model are compared with experimental results provided by Bridge [4], Shakir-Khalil and Zeghiche [5] and Matsui et al. [6]. Fig. 1 shows the load-deflection curves for specimen SCH2 predicted by the numerical model developed by Patel et al. [15] and obtained from the experiments conducted by Bridge [4]. It can be observed that the load-deflection curve predicted by the numerical model is in good agreement with the experimental results. The difference between the experimental and numerical ultimate axial load is only 1.0%. Fig. 2 gives the predicted and experimental axial load-deflection curves for specimen R5 tested by Shakir-Khalil and Zeghiche [5]. It can be seen that the numerical model predicts well the

load-deflection curve for the tested specimen up to the ultimate axial load. However, the computed ultimate load is slightly higher than the experimental value due to the uncertainty of the initial imperfections and material properties.

Fig. 3 presents a comparison between the numerical and experimental axial load-deflection curves for specimen S3. The figure shows that the numerical and experimental axial load-deflection curves are almost identical up to the ultimate load. The ultimate axial strength predicted by the numerical model is 98% of the experimental value. The verification of the numerical model shows that the numerical model yields good predictions of the axial load-deflection and axial load-moment interaction curves for normal and high strength CFST slender beam-columns.

3. Parametric study

An extensive parametric study was performed to investigate the influences of local buckling of the steel tube, column slenderness ratio, depth-to-thickness ratio, eccentricity ratio, concrete compressive strengths and steel yield strengths on the fundamental behavior of full-scale high strength thin-walled rectangular CFST slender beam-columns under axial load and unixial bending. Only one variable was considered at a time to assess its individual effect.

3.1 Influences of local buckling

The numerical model was employed to study the effects of local buckling on the behavior of high strength rectangular CFST slender beam-columns. A thin-walled CFST beam-column with a cross-section of 700 × 700 mm was considered. The thickness of the steel tube was 70

mm so that its depth-to-thickness ratio (D/t) was 100. The yield and tensile strengths of the steel tube were 690 MPa and 790 MPa respectively while its Young's modulus was 200 GPa. High strength concrete with compressive strength of 70 MPa was filled into the steel tube. The column slenderness ratio (L/r) was 40. The axial load was applied at an eccentricity 70 mm so that the loading eccentricity ratio (e/D) was 0.1. The initial geometric imperfection at the mid-height of the beam-column was assumed to be $L/1500$. The slender beam-column was analyzed by considering and ignoring local buckling effects respectively.

The influences of local buckling on the axial load-deflection curves for high strength thin-walled CFST slender beam-columns are shown in Fig. 4. It can be seen from Fig. 4 that local buckling remarkably reduces the ultimate axial load of the slender beam-column under eccentric loading. The ultimate axial load of the slender beam-column is overestimated by 8.32% if the local buckling of the steel tube was not considered. Therefore, it is important to incorporate local buckling effects in the nonlinear inelastic analysis of rectangular thin-walled CFST slender beam-columns especially those made of high strength thin-walled steel tubes in order to accurately predict the behavior of such columns.

Fig. 5 demonstrates the influences of local buckling on the axial load–moment interaction diagram for the CFST slender beam-column. As shown in Fig. 5, the ultimate axial strength was normalized by the ultimate axial load (P_{oa}) of the axially loaded slender column including local buckling effects, while the ultimate moment was normalized by the ultimate pure bending moment (M_o) of the slender beam-column with local buckling effects. It can be observed from Fig. 5 that local buckling considerably reduces the ultimate strength of the slender beam-column. If local buckling was not considered in the numerical analysis, the

ultimate pure bending strength of the slender beam-column is overestimated by 5.02% while the ultimate bending strength of the slender beam-column is overestimated by 7.49%.

3.2 Influences of column slenderness ratio

The numerical model developed was used to examine the effects of the column slenderness ratio (L/r) which is an important parameter that influences the behavior of CFST beam-columns. High strength thin-walled CFST slender beam-columns with a cross-section of 600×600 mm were considered. The depth-to-thickness ratio of the section was 50. Column slenderness ratios (L/r) of 22, 50, 65 and 80 were considered in the parametric study. The loading eccentricity ratio (e/D) of 0.1 was specified in the analysis of slender beam-columns with various L/r ratios. The initial geometric imperfection of $L/1500$ at the mid-height of the beam-columns was incorporated in the model. The beam-columns were made of high strength steel tubes with the yield and tensile strengths of 690 MPa and 790 MPa respectively. The Young's modulus of the steel tubes was 200 GPa. The steel tubes were filled with high strength concrete of 80 MPa.

Fig. 6 presents the axial load-deflection curves for the beam-columns with various slenderness ratios. It appears that the ultimate axial load is strongly affected by the column slenderness ratio. Increasing the column slenderness ratio significantly reduces its ultimate axial load. Columns with a smaller slenderness ratio are shown to be less ductile than the ones with a larger slenderness ratio. The mid-height deflection at the ultimate axial strength of the beam-columns increases with increasing the column slenderness ratio. Fig. 7 shows the ratio of the ultimate axial load (P_n) to the ultimate axial strength (P_{oa}) of the column's section under eccentric loading as a function of the column slenderness ratio. As demonstrated in Fig. 7, the

ultimate axial strength of the beam-column with a L/r ratio of 22 is 99% of the section's strength.

Fig. 8 demonstrates the effects of the column slenderness ratio on the axial load-moment strength interaction curves for CFST beam-columns. In Fig. 8, the ultimate axial strength (P_n) was normalized to the ultimate axial load (P_o) of the axially loaded beam-column section while the ultimate moment (M_n) was normalized to the ultimate pure bending moment (M_o) of the beam-column. The column slenderness ratio $L/r = 0$ was used in the axial load-moment interaction analysis to determine the ultimate strengths of the composite section. It can be seen from Fig. 8 that reducing the column L/r ratio enlarges the axial load-moment interaction diagram. The ultimate bending strength of the beam-column is shown to decrease as the column slenderness ratio increases.

3.3 Influences of depth-to-thickness ratio

Local buckling of a thin-walled steel tubes depends on its depth-to-thickness ratio (D/t). The numerical model was utilized to examine the effects of D/t ratio on the load-deflection and axial load-moment interaction curves for high strength CFST slender beam-columns. A square cross-section of 650 × 650 mm was considered in the analysis. The D/t ratios of the column sections were calculated as 40, 60, 80 and 100 by changing the thickness of the steel tubes. The column slenderness ratio (L/r) was 35. The loading eccentricity ratio (e/D) was taken as 0.1 in the analysis. The initial geometric imperfection of the beam-columns at mid-height was specified as $L/1500$. The yield and tensile strengths of the steel tubes were 690

MPa and 790 MPa respectively while the Young's modulus of the steel tubes was 200 GPa. The compressive strength of the in-filled concrete was 60 MPa.

The influences of D/t ratio on the axial load-deflection curves for high strength thin-walled CFST slender beam-columns are illustrated in Fig. 9. The figure shows that increasing the D/t ratio of the slender beam-columns slightly reduces their initial stiffness. However, increasing the D/t ratio significantly reduces the ultimate axial strength of eccentrically loaded CFST slender beam-columns. This is attributed to the fact that a column section with a larger D/t ratio has a lesser steel area and it may undergone local buckling which reduces the ultimate strength of the column.

Fig. 10 demonstrates the influence of D/t ratio on the axial load-moment interaction diagrams for high strength thin-walled CFST slender beam-columns. In each interaction curve, the axial load (P_n) was divided by the ultimate axial strength (P_{oa}) of the axially loaded slender beam-column, while the moment (M_n) was divided by the ultimate pure bending moment (M_o) of the beam-column. It can be seen from Fig. 10 that decreasing the D/t ratio of the slender beam-column narrows the axial load-moment interaction diagram for the slender beam-column. In addition, the flexural strength at the maximum moment point is shown to increase remarkably with increasing the D/t ratio.

3.4 Influences of loading eccentricity ratio

The fundamental behavior of a rectangular CFST slender beam-column under axial load and uniaxial bending is influenced by the loading eccentricity ratio (e/D). To investigate this

effect, a beam-column with a cross-section of 600 × 700 mm and loading eccentricity ranged from 0.1 to 0.2, 0.4 and 0.6 were analyzed using the numerical model. The depth-to-thickness ratio of the section was 60. The slenderness ratio (L/r) of the beam-column was 30. The initial geometric imperfection of the beam-column at the mid-height was assumed to be $L/1500$. The yield and tensile strengths of the steel tubes were 690 MPa and 790 MPa respectively. The beam-column was filled with high strength concrete of 90 MPa. The Young's modulus of 200 GPa was specified for the steel tubes in the analysis.

The computed axial load-deflection curves for high strength rectangular CFST slender beam-columns with different loading eccentricity ratios are presented in Fig. 11. It can be seen that the initial stiffness of the slender beam-columns decreases with an increase in the e/D ratio. In addition, increasing the e/D ratio significantly reduces the ultimate loads of the beam-columns. This is attributed to the fact that increasing the e/D ratio increases the bending moments at the column ends which significantly reduce the ultimate axial load of the slender beam-columns. Furthermore, the mid-height deflections at the maximum axial load of the slender beam-column increase with an increase in the eccentricity ratio. The displacement ductility of a slender beam-column is shown to be improved when increasing the eccentricity ratio. Fig. 12 shows that the ultimate axial load is a function of the loading eccentric ratio. The figure clearly shows that the effect of the loading eccentricity ratio on the ultimate axial strengths of CFST slender bean-columns is significant.

3.5 Influences of concrete compressive strengths

The effects of concrete compressive strengths on the strengths and behavior of high strength CFST slender beam-columns with local buckling effects were studied by the numerical

model. In the parametric study, the concrete compressive strength was varied from 60 MPa to 100 MPa. The width and depth of the steel tube was 600 mm and 800 mm respectively. The steel tube wall was 10 mm thick so that its depth-to-thickness ratio (D/t) was 80. The slenderness ratio (L/r) of the beam-column was 32. The initial geometric imperfection of the beam-column at the mid-height was taken as $L/1500$. The loading eccentricity ratio (e/D) was 0.1. The steel yield and ultimate tensile strengths were 690 MPa and 790 MPa respectively and the Young's modulus of the steel tubes was 200 GPa.

The axial load-deflection curves for high strength rectangular CFST slender beam-columns with different concrete strengths are depicted in Fig. 13. It would appear from Fig. 13 that the ultimate axial strengths of rectangular CFST slender beam-columns increase significantly with an increase in the concrete compressive strength. Increasing the concrete compressive strength from 60 MPa to 80 MPa and 100 MPa increases the ultimate axial strength by18.13% and 35.84%, respectively. It can be seen from Fig. 13 that increasing the concrete compressive strength results in a slight increase in the initial stiffness of the slender beam-columns.

The normalized axial load-moment interaction diagrams for rectangular CFST slender beam-columns are given in Fig. 14. It can be observed that increasing the concrete compressive strength enlarges the $P-M$ interaction curves. The ultimate bending moment of the slender beam-columns is found to increase considerably with increasing the concrete compressive strength. By increasing the concrete compressive strength from 60MPa to 80MPa and 100 MPa, the ultimate bending moment of the column is increased by 7.23% and 13.87%, respectively. The ultimate pure bending strengths of rectangular CFST beam-columns are also found to increase with an increase in the compressive strength of the in-filled concrete.

3.6 Influences of steel yield strengths

Rectangular thin-walled CFST slender beam-columns with different steel yield strengths and a cross-section of 700 × 800 mm were analyzed using the numerical model. The depth-to-thickness (D/t) ratio of the section was 70. The yield strengths of the steel tubes were 500 MPa, 600 MPa and 690 MPa and the corresponding tensile strengths were 590 MPa, 690 MPa and 790 MPa, respectively. The column slenderness ratio (L/r) of 45 was used in the parametric study with a loading eccentricity ratio (e/D) of 0.1. The initial geometric imperfection of the beam-column at the mid-height was taken as $L/1500$. The Young's modulus of steel was 200 GPa. The steel tubes were filled with 100 MPa concrete.

Fig. 15 illustrates the influences of steel yield strengths on the axial load-deflection curves for high strength rectangular CFST slender beam-columns. It can be observed from Fig. 15 that the steel yield strength does not have an effect on the initial stiffness of the beam-columns. However, the ultimate axial strength of slender beam-columns is found to increase significantly with an increase in the steel yield strength. By increasing the steel yield strength from 500 MPa to 600 MPa and 690 MPa, the ultimate axial load of the slender beam-column is found to increase by 4.92% and 8.95% respectively.

The normalized axial load-moment interaction diagrams for rectangular CFST beam-columns made of different strength steel tubes are presented in Fig. 16. The figure shows that the normalized axial load-moment interaction curve is enlarged by reducing the steel yield strength. In addition, the ultimate bending strength of the slender beam-column increases by 13.61% and 28.07%, when increasing the steel yield strength from 500 MPa to 600 MPa and 690 MPa, respectively. The ultimate pure bending strength of the slender beam-columns

increases significantly with increasing the steel yield strength. When increasing the steel yield strength from 500 MPa to 600 MPa and 690 MPa, the ultimate pure bending moment of the slender beam-columns is increased by 13.15% and 28.35% respectively.

4. Conclusions

The verification and applications of a numerical model developed for the nonlinear inelastic analysis of high strength thin-walled rectangular CFST slender beam-columns with local buckling effects have been presented in this paper. The numerical model was verified by comparisons of computational solutions with experimental results of normal and high strength CFST slender beam-columns presented by independent researchers. It has been demonstrated that the numerical model developed can yield accurate predictions of the axial load-deflection and axial load-moment interaction curves for high strength rectangular CFST slender beam-columns with local buckling effects. This paper has provided new numerical results on the fundamental behavior of full-scale high strength thin-walled rectangular steel slender tubes filled with high strength concrete with various parameters including the effects of local buckling, column slenderness ratio, depth-to-thickness ratio, loading eccentricity ratio, concrete compressive strengths and steel yield strengths. The numerical results presented can be used to validate other nonlinear inelastic analysis techniques and to develop composite design codes for high strength thin-walled rectangular CFST slender beam-columns. Furthermore, the numerical model developed can be used in the analysis and design of normal and high strength CFST slender columns subjected to axial load and uniaxial bending in practice.

References

[1] EN 1994-1-1, Eurocode 4: design of composite steel and concrete structures. Part 1-1, General rules and rules for buildings, CEN 2004.

[2] LRFD. Load and Resistance Factor Design Specification for Steel Buildings. American Institution of Steel Construction, 1999.

[3] ACI-318. Building Code Requirements for Reinforced Concrete. Detroit (MI); ACI, 2005.

[4] Bridge RQ. Concrete filled steel tubular columns. School of Civil Engineering, The University of Sydney, Sydney, Australia, 1976, Research Report No. R 283.

[5] Shakir-Khalil H, Zeghiche J. Experimental behavior of concrete-filled rolled rectangular hollow-section columns. The Structural Engineer 1989; 67(3): 346-53.

[6] Matsui C, Tsuda K, Ishibashi Y. Slender concrete filled steel tubular columns under combined compression and bending. Proceedings of the 4th Pacific Structural Steel Conference, Pergamon, Singapore 1995; 3(10): 29-36.

[7] Chung J, Tsuda K, Matsui C. High-strength concrete filled square tube columns subjected to axial loading. The Seventh East Asia-Pacific Conference on Structural Engineering & Construction, Kochi, Japan 1999; Volume 2:955-60.

[8] Vrcelj Z, Uy B. Behaviour and design of steel square hollow sections filled with high strength concrete. Australian Journal of Structural Engineering 2002; 3(3): 153-70.

[9] Zhang S, Guo L, Tian H. Eccentrically loaded high strength concrete-filled square steel tubes. Proceedings of the International Conference on Advances in Structures, Sydney, Australia 2003; ASSCCA 03: 987-93.

[10] Lakshmi B, Shanmugam NE. Nonlinear analysis of in-filled steel-concrete composite columns. Journal Structural Engineering, ASCE 2002; 128(7):922-33

[11] Liang QQ. Performance-based analysis of concrete-filled steel tubular beam-columns, Part I: Theory and algorithms. Journal of Constructional Steel Research 2009; 65(2): 363-72.

[12] Liang QQ. Performance-based analysis of concrete-filled steel tubular beam-columns, Part II: Verification and applications. Journal of Constructional Steel Research 2009; 65(2):351-62.

[13] Liang QQ. High strength circular concrete-filled steel tubular slender beam-columns, Part I: Numerical analysis. Journal of Constructional Steel research 2011; 67(2):164-71.

[14] Liang QQ. High strength circular concrete-filled steel tubular slender beam-columns, Part II: Fundamental behavior. Journal of Constructional Steel Research 2011; 67(2):172-80.

[15] Patel VI, Liang QQ, Hadi MNS. High strength thin-walled rectangular concrete-filled steel tubular slender beam-columns, Part I: Modeling. Journal of Constructional Steel Research 2011 (submitted).

Figures and Tables

Table 1. Ultimate axial strengths of normal strength CFST slender beam-columns.

Specimens	$B\times D\times t$ (mm)	D/t	L (mm)	e_x (mm)	e_y (mm)	u_o (mm)	f_c' (MP)	f_{sy} (MPa)	f_{su} (MPa)	E_s (GPa)	$P_{u.\exp}$ (kN)	$P_{u.\text{num}}$ (kN)	$\frac{P_{u.\text{num}}}{P_{u.\exp}}$
SCH-1	203.7× 203.9 × 9.96	20	2130	0	38	1.19	29.9	291	410	205	1956	1995.73	1.02
SCH-2	204.0 ×203.3 × 10.01	20	3050	0	0	1.40	31.1	290	410	205	2869	2907.4	1.01
SCH-7	152.5 ×152.3 × 6.48	24	3050	0	38	0.51	31.1	254	410	205	680	734.0	1.08
R1	80× 120 × 5	24	3210	0	0		37.4	386.3	430	205	600	600.41	1.00
R2	80× 120 × 5	24	3210	0	24		34.0	386.3	430	205	393	383.61	0.98
R5	80× 120 × 5	24	2940	40	0		36.6	343.3	430	205	210	216.24	1.03
S1	149.8× 149.8 × 4.27	35	2700	0	0		31.9	445	498	200	1355	1356.99	1.00
S2	149.8× 149.8 × 4.27	35	2700	0	25		31.9	445	498	200	847	868.80	1.03
S3	149.8× 149.8 × 4.27	35	2700	0	75		31.9	445	498	200	552	542.20	0.98
S4	149.8× 149.8 × 4.27	35	2700	0	125		31.9	445	498	200	383	393.13	1.03
S5	149.8× 149.8 × 4.27	35	3600	0	0		31.9	445	498	200	1143	1140.86	1.00
S6	149.8× 149.8 × 4.27	35	3600	0	25		31.9	445	498	200	706	734.41	1.04
S7	149.8× 149.8 × 4.27	35	3600	0	75		31.9	445	498	200	440	464.39	1.06
S8	149.8× 149.8 × 4.27	35	3600	0	125		31.9	445	498	200	325	346.85	1.07
S9	149.8× 149.8 × 4.27	35	4500	0	0		31.9	445	498	200	909	895.88	0.99
S10	149.8× 149.8 × 4.27	35	4500	0	25		31.9	445	498	200	588	602.78	1.03
S11	149.8× 149.8 × 4.27	35	4500	0	75		31.9	445	498	200	374	394.64	1.06
S12	149.8× 149.8 × 4.27	35	4500	0	125		31.9	445	498	200	278	302.98	1.09
Mean													1.03
Standard deviation (SD)													0.03
Coefficient of variation (COV)													0.03

Table 2. Ultimate axial strengths of high strength CFST slender beam-columns.

Specimens	$B\times D\times t$ (mm)	D/t	L (mm)	e_x (mm)	e_y (mm)	f_c' (MP)	f_{sy} (MPa)	f_{su} (MPa)	E_s (GPa)	$P_{u.\exp}$ (kN)	$P_{u.\text{num}}$ (kN)	$\frac{P_{u.\text{num}}}{P_{u.\exp}}$
C18-1	125× 125 × 3.2	39	2250	0	20.5	94.1	450	528	200	830	874.28	1.05
C18-3	125× 125 × 3.2	39	2250	0	61.5	94.1	450	528	200	457	490.57	1.07
C24-0	125× 125 × 3.2	39	3000	0	0	94.1	450	528	200	1079	1108.18	1.03
C24-1	125× 125 × 3.2	39	3000	0	20.5	94.1	450	528	200	664	676.12	1.02
C24-3	125× 125 × 3.2	39	3000	0	61.5	94.1	450	528	200	375	399.06	1.06
C30-0	125× 125 × 3.2	39	3750	0	0	94.1	450	528	200	747	814.05	1.09
CCH1	75× 75 × 3	25	1770	0	3.75	79	450	530	193.7	414	393.61	0.95
CCH2	65× 65 × 3	22	1770	0	3.25	79	400	530	189.3	294	263.12	0.89
CCM1	75× 75 × 3	25	1770	0	3.75	52	450	530	193.7	343	355.98	1.04
CCM2	65× 65 × 3	22	1770	0	3.25	52	400	530	189.3	269	242.59	0.90
Mean												1.01
Standard deviation (SD)												0.07
Coefficient of variation(COV)												0.07

Table 3. Ultimate bending strengths of rectangular CFST slender beam-columns under eccentric loading.

Specimens	$B\times D\times t$ (mm)	D/t	L (mm)	e_x (mm)	e_y (mm)	u_o (mm)	f_c' (MP)	f_{sy} (MPa)	f_{su} (MPa)	E_s (GPa)	$M_{n.\exp}$ (kNm)	$M_{n.\text{num}}$ (kNm)	$\frac{M_{n.\text{num}}}{M_{n.\exp}}$
SCH-1	203.7× 203.9 × 9.96	20	2130	0	38	1.19	29.9	291	410	205	74.33	79.12	1.06
R2	80× 120 × 5	24	3210	0	24		34.0	386.3	430	205	9.43	8.76	0.93
R5	80× 120 × 5	24	2940	40	0		36.6	343.3	430	205	8.4	8.82	1.05
S2	149.8× 149.8 × 4.27	35	2700	0	25		31.9	445	498	200	21.18	22.85	1.08
S3	149.8× 149.8 × 4.27	35	2700	0	75		31.9	445	498	200	41.4	39.99	0.97
S4	149.8× 149.8 × 4.27	35	2700	0	125		31.9	445	498	200	47.88	49.57	1.04
S10	149.8× 149.8 × 4.27	35	4500	0	25		31.9	445	498	200	14.7	15.89	1.08
C24-1	125× 125 × 3.2	39	3000	0	20.5		94.1	450	528	200	13.61	14.29	1.05
Mean													1.03
Standard deviation (SD)													0.05
Coefficient of variation (COV)													0.05

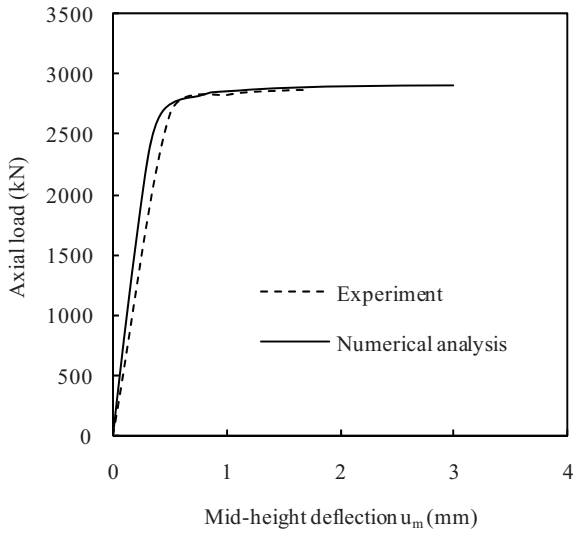

Fig. 1. Comparison of predicted and experimental axial load-deflection curves for specimen SCH-2.

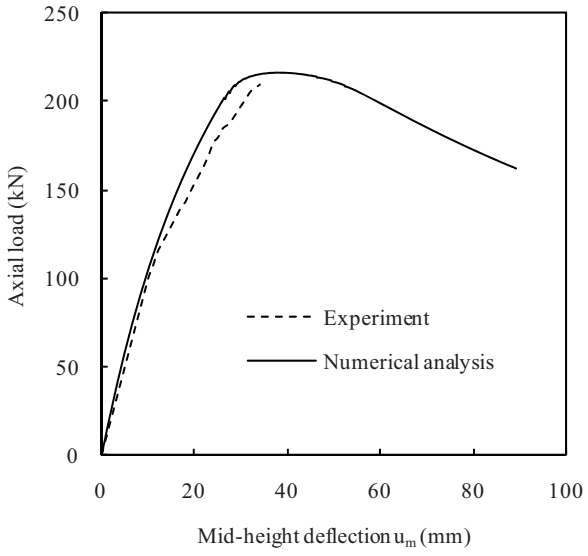

Fig. 2. Comparison of predicted and experimental axial load-deflection curves for specimen R5.

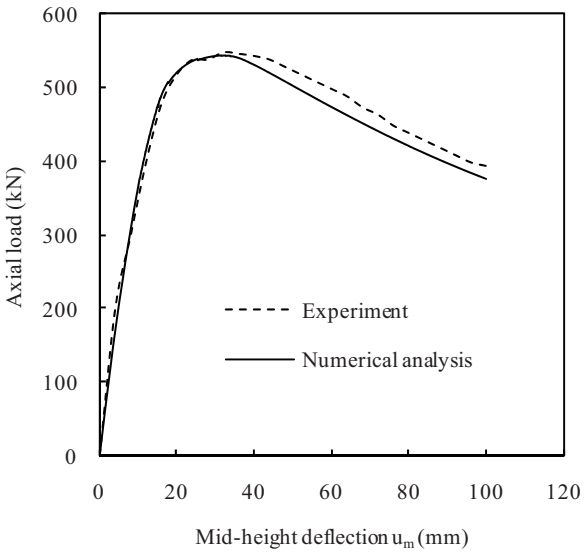

Fig. 3. Comparison of predicted and experimental axial load-deflection curves for specimen S3.

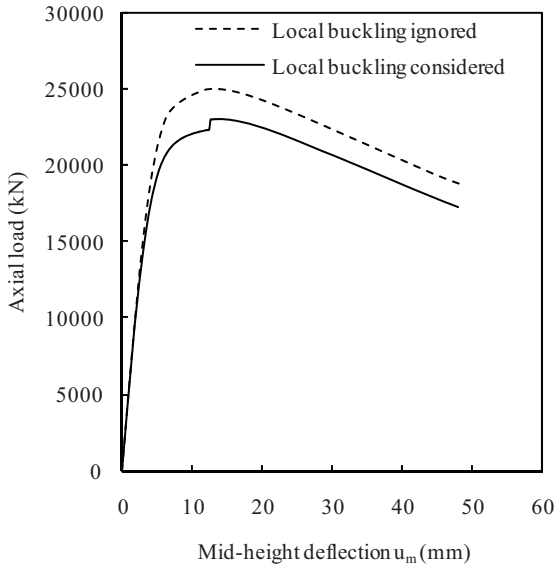

Fig. 4. Influence of local buckling on the axial load-deflection curves for thin-walled CFST slender beam-columns.

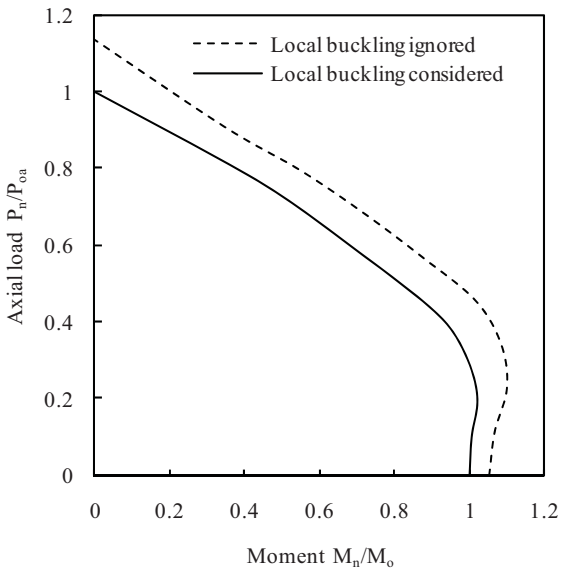

Fig. 5. Influence of local buckling on the axial load-moment interaction diagrams for thin-walled CFST slender beam-columns.

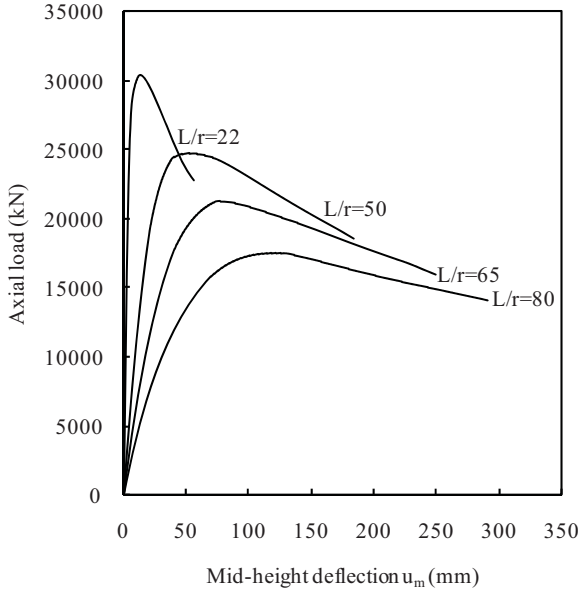

Fig. 6. Influence of column slenderness ratio on the axial load-deflection curves for thin-walled CFST slender beam-columns.

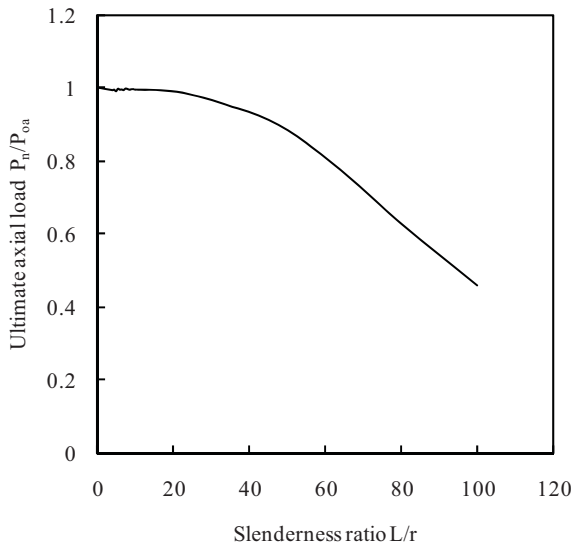

Fig. 7. Influence of column slenderness ratio on the ultimate axial loads of thin-walled CFST slender beam-columns.

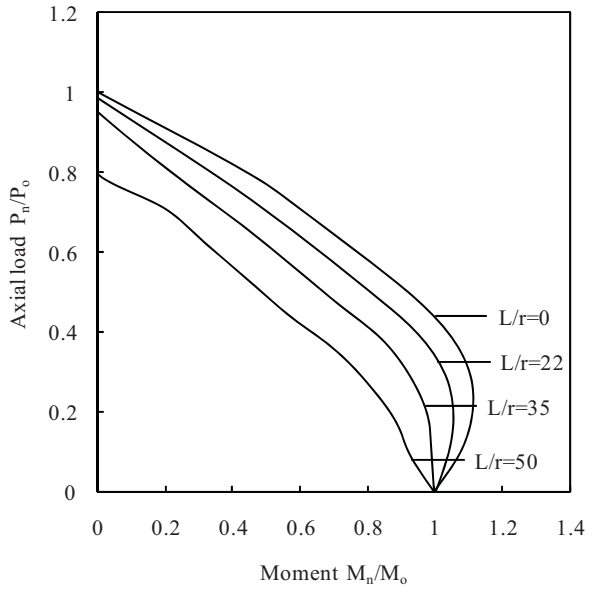

Fig. 8. Influence of column slenderness ratio on the axial load-moment interaction diagrams for thin-walled CFST slender beam-columns.

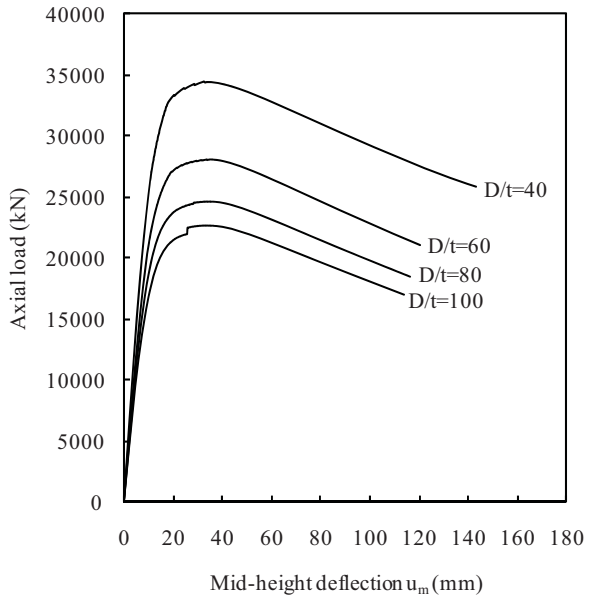

Fig. 9. Influence of D/t ratio on the axial load-deflection curves for thin-walled CFST slender beam-columns.

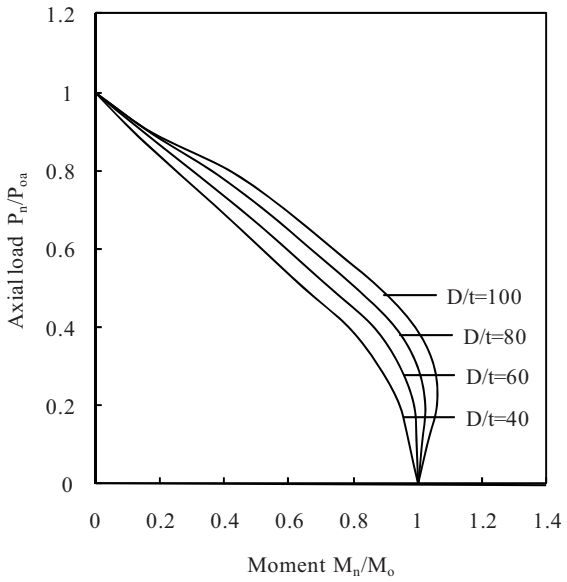

Fig. 10. Influence of D/t ratio on the axial load-moment interaction diagrams for thin-walled CFST slender beam-columns.

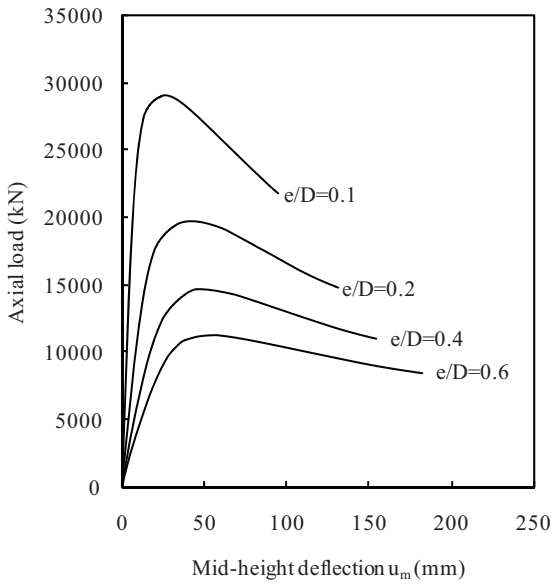

Fig. 11. Influence of loading eccentricity ratio on the axial load-deflection curves for thin-walled CFST slender beam-columns.

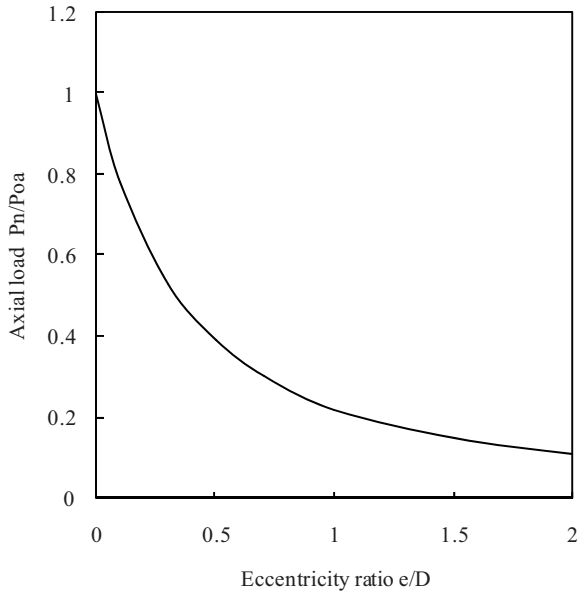

Fig. 12. Influence of loading eccentricity ratio on the ultimate axial loads of thin-walled CFST slender beam-columns.

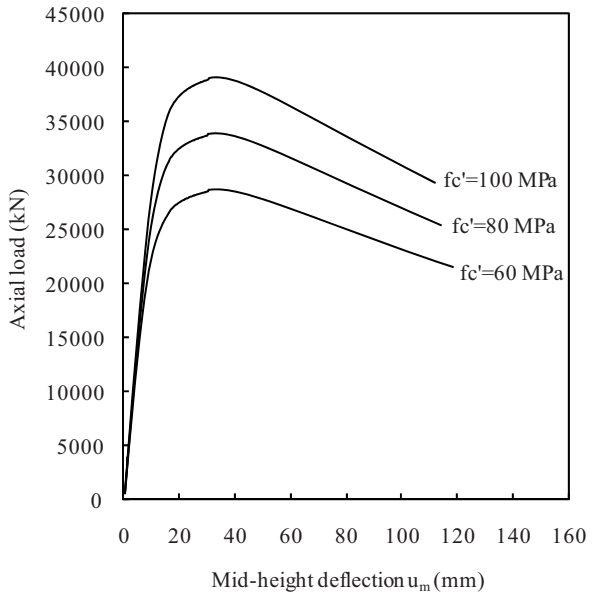

Fig. 13. Influence of concrete compressive strenghts on the axial load-deflection curves for thin-walled CFST slender beam-columns.

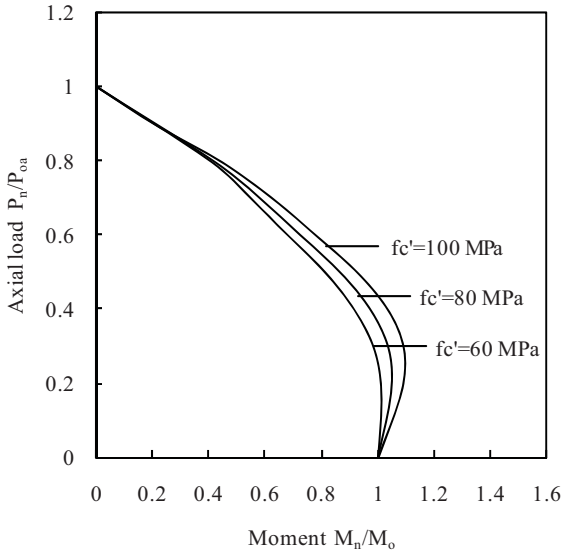

Fig. 14. Influence of concrete compressive strengths on the axial load-moment interaction diagrams for thin-walled CFST slender beam-columns.

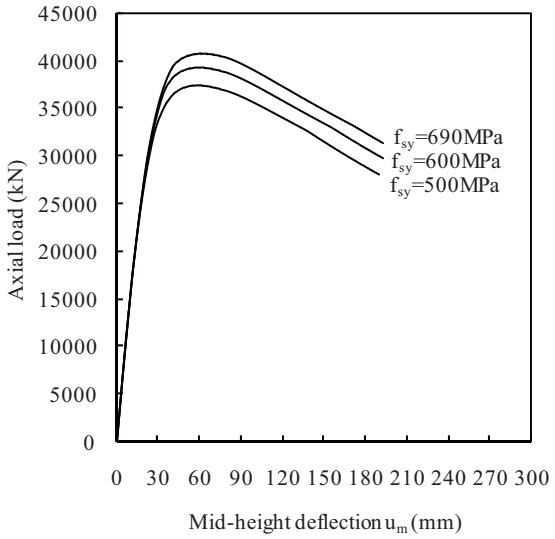

Fig. 15. Influence of steel yield strenghts on the axial load-deflection curves for thin-walled CFST slender beam-columns.

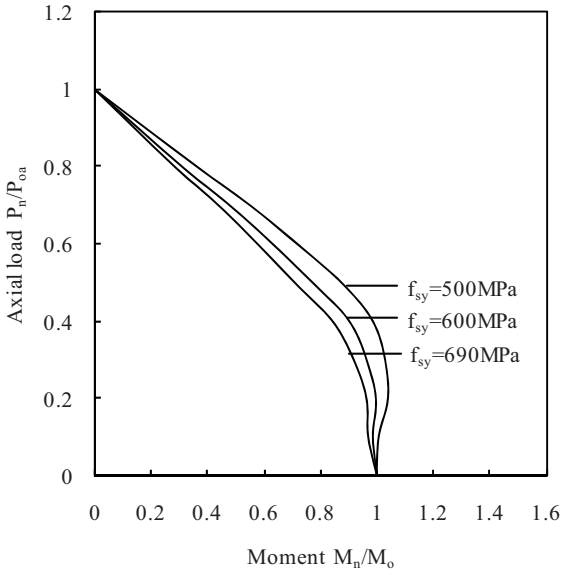

Fig. 16. Influence of steel yield strengths on the axial load-moment interaction diagrams for thin-walled CFST slender beam-columns.